Selective leaching of vanadium from calcification-roasted pellets of vanadium-titanium-iron concentrate by a cyclic two-stage sulfuric acid process

Zhonghui Peng [1,2], Zhixiang Wang [1,*], Yang Li [1], Yongze Zhu [1], Keqiang Xie [1,*]

[1] Faculty of Metallurgical and Energy Engineering, Kunming University of Science and Technology, Kunming 650093, China

[2] Sichuan Lomon Mining and Metallurgy Co., Ltd, Panzhihua 617100, China

* Correspondence: 164163323@qq.com (Z.Wang); xkqzhh@sina.com (K.Xie)

Abstract

Here, a process for leaching vanadium from calcified roasting pellets (CPVC) of vanadium-titanium iron concentrate by a two-stage sulfuric acid cycle was proposed. When the silicon removal acid concentration of the pellet in the first stage was 1.5 mol/L, the solid-liquid ratio was 6: 1, the silicon removal acid concentration of the leaching solution was 3.0 mol/L, and the standing time was 48 h, the silica gel formation time was 23 h, the filtration time was 70 s, and the loss rates of vanadium and iron were 1.52% and 0.17%, respectively. When the acid concentration was 2 mol/L, at room temperature, using a leaching time of 28 days, and a solid-liquid ratio of 5: 1 in the second stage, the total leaching rates of vanadium and iron were 75.52% and 0.71%, respectively. The concentration of vanadium in the leaching solution reached 6.80 g/L, and vanadium was directly precipitated without extraction. After secondary roasting, the crushing strength of the pellets reached 2250 N, which met the requirement for blast furnace iron making. The Eh-pH diagrams of the V-Fe-H_2O system at different temperatures were plotted. Thermodynamically, it was difficult to selectively leach vanadium and iron by changing the conventional acid leaching conditions. In addition, the pellets before and after leaching were analyzed. The grade of iron in the pellets increased slightly after leaching, and the main phases in the pellets remained as Fe_2O_3 and Fe_9TiO_{15}. The S in the sulfuric acid solution entered the leached pellets during the acid leaching reaction and was removed by the secondary roasting of the leached pellets.

Keywords: Vanadium-titanium-iron concentrate; Pellet; Sulfuric acid; Cyclic leaching; Vanadium; Eh-pH diagrams

1. Introduction

Vanadium (V) is an important transition metal that accounts for 0.02% of the total mass of the earth's crust and is a prevalent element in the natural environment [1,2]. Due to its physical properties, it is widely used in steel alloys, chemicals, batteries, and pharmaceuticals [3,4]. China has the world's largest vanadium reserves, among which vanadium-titanium magnetite resources are the most abundant and are mainly distributed in the Panzhihua-Xichang area of Sichuan [5]. Approximately 88% of global V production comes from vanadium and titanium magnetite.[6] Vanadium-titanium-iron concentrate is obtained from the beneficiation of vanadium-titanium magnetite, in which vanadium is homogeneously present in titanium magnetite and displaces high-valent iron ions. Titanium magnetite is a composite of host crystals (Fe_3O_4), chadacrysts (ferro-ortho-titanate $2FeO\cdot TiO_2$, titanic iron ore $FeO\cdot TiO_2$, pseudobrookite ($FeO\cdot 2TiO_2$), and alumina-magnesia spinel (Mg, Fe)(Al, Fe)$_2$O$_4$) [6,7].

The process for extracting vanadium from vanadium titanomagnetite in China is to obtain vanadium slag from vanadium titanomagnetite smelted by blast furnaces with ferro-vanadium blown in a converter. This is then subjected to sodium or calcium roasting in a rotary kiln, followed by water or acid leaching, purification, and vanadium precipitation [8]. Although this process is compatible with the steel smelting process, it results in a low total vanadium yield and several toxic substances in vanadium slag [9]. Direct vanadium extraction methods from vanadium-containing raw materials have been heavily researched in recent years and include sodium roasting, salt-free roasting, direct acid leaching, sub-molten salt technology, and calcification roasting with acid or alkaline leaching [10]. Sodium roasting is a more mature technology, but the vanadium phase conversion is low, the introduction of sodium salts adversely affects the subsequent ironmaking, corrodes equipment, and pollutes the air [11]. Calcification roasting-alkali leaching is seldom used, the strong alkali leaching effect is not ideal, and the costs are too high [12]. Salt-free roasting-leaching uses a high roasting temperature that results in the serious loss of vanadium due to evaporation [13]. Sulfuric acid direct leaching uses simple equipment and is environmentally friendly, but its leaching efficiency is low and requires the addition of a leaching aid to help destroy the vanadium-containing phases [14]. Sub-molten salt technology is used to leach vanadium, but this process consumes large amounts of alkali agents and energy

[15]. Many new processes have also been used to leach vanadium, such as manganese salt roasting acid leaching, microwave roasting, electrooxidation acid leaching, and liquid oxidation. However, for various reasons, these methods have hardly been used industrially [16,17]. Calcification roasting acid leaching does not discharge corrosive gases, has less wastewater discharge, and produces easily-treatable extraction tailings [18]. Wen et al [19]. studied the calcification roasting acid leaching of vanadium. The introduction of a calcium salt formed calcium sulfate during leaching that wrapped the unreacted vanadium-containing phase, reduced the recovery of vanadium, and also contained a by-product that was difficult to reuse. Zhang et al [20]. studied the calcification roasting acid leaching of vanadium and showed that vanadium and iron were simultaneously leached. In summary, calcification roasting sulfuric acid leaching mainly has two defects. The calcium salt added during roasting precipitates as $CaSO_4$ during acid leaching, which coats on the surface of the raw material to hinder leaching [21]. The leaching process is also non-selective and, although V is leached, large quantities of valuable metals such as Fe and Ti are also leached, which complicates the selective extraction and precipitation of vanadium [22].

Due to the above situation, this study proposed a two-stage cyclic leaching method for CPVC with sulfuric acid. The process involves two stages. The first stage of leaching includes the removal of silicon from the pellet and silicon solution removal. In the second stage of leaching, sulfuric acid solution was used for the cyclic leaching of silicon-removal pellets. The influence of $CaSO_4$ on leaching was investigated by pelletizing and circulating leaching. Selective vanadium leaching was achieved, and the final leaching rates of vanadium and iron were 75.52% and 0.71%, respectively. After secondary roasting, the crushing strength of the pellets reached 2250 N. The advantage of this process is that the iron is retained in pellets, while vanadium is extracted. The leached pellets met the requirements for blast furnace ironmaking and the crushing strength of pellets after secondary roasting. In addition, due to the large solid-liquid ratio, the vanadium concentration in the leaching solution reached 6.80 g/L. Subsequent vanadium extraction did not require a separate extraction step because vanadium directly precipitated, which significantly improved the production efficiency.

2. Materials and methods

2.1 Materials

The raw material used in this study was CPVC, which was provided by Sichuan Longmang Mining and Metallurgy Co., Ltd. The phase analysis of the raw material was carried out by X-ray fluorescence spectroscopy (XRF), and the results are shown in Table 1. The main elements in CPVC were Fe and Ti. There were also small amounts of impurities such as Si, Ca, Mg, Al, Cr, and the content of V was only 0.3%. Analytically pure sulfuric acid was provided by Chengdu Kelong Chemical Reagent Factory, and industrial flocculant was provided by Dezhou Ruixing Water Purification Raw Materials Co., Ltd.

Table 1 Main components of vanadium titanomagnetite.

Element	Fe	Ti	Si	Ca	Mg	Al	Cr	V	Ni	Mn
Content / wt%	45.0	8.0	2.0	2.0	1.0	1.0	0.5	0.3	0.2	0.2

2.2 Experimental procedure

The leaching experiment was conducted under atmospheric pressure, as shown in Figure. 1. CPVC was stored in a custom container, heated in a large-mouth jar with dilute sulfuric acid solution through a thermostatic water bath. The customized reaction container was fixed directly above the jar with clips. The circulation of dilute sulfuric acid solution between the custom container and large-mouth jar was realized by a peristaltic pump. The first stage of leaching involved optimizing the silicon removal of acid leaching pellets under four different acid concentrations (0.4 mol/L, 0.8 mol/L, 1.0 mol/L, 1.5 mol/L) and four different solid-liquid ratios (3: 1, 4: 1, 5: 1, 6: 1). The silicon removal using the acid leaching solution was optimized under four different acid concentrations (1.5 mol/L, 2.0 mol/L, 2.5 mol/L, 3.0 mol/L) and four different standing times (36 h, 48 h, 60 h, 72 h). The pellets and leachate with their silicon removed during the first leaching stage were mixed. To optimize the leaching rate of V and Fe, the second stage leaching involved the use of four different acid concentrations (1.0 mol/L, 1.5 mol/L, 2.0 mol/L, 2.5 mol/L), four different leaching times (6 d, 8 d, 10 d, 12 d), four different solid-liquid ratios (3: 1, 4: 1, 5: 1, 6: 1), and four different leaching temperatures (room temperature, 40 ℃, 50 ℃, 60 ℃).

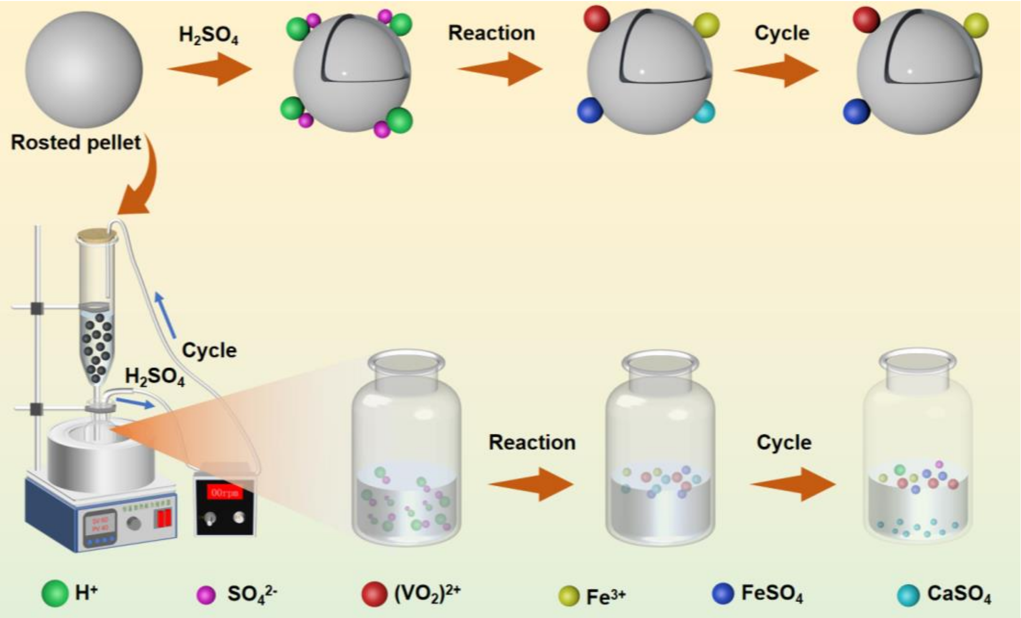

Fig. 1. Experimental reaction mechanism diagram

2.3. Characterization and analysis

X-ray diffraction (XRD, Panalytical Empyrean) was used to analyze the phase composition of the roasted and leached pellets. X-ray fluorescence spectroscopy (XRF) was used to analyze the chemical composition of roasted pellets and leached pellets. X-ray photoelectron spectroscopy (XPS) was used to analyze the phase changes of V and Fe. Scanning electron microscopy (SEM, Quanta Q 400, FEI Company, Hillsboro, OR, USA) for observations and for the elemental analysis of roasted and leached pellets. The strength of pellets after two-stage leaching and secondary roasting was measured by a universal testing machine (WE-100). The concentration of vanadium in the solution was determined by ferrous ammonium sulfate titration. The concentrations of other elements were determined by inductively coupled plasma-atomic emission spectrometry (ICP-AES, Optima8000).

3. Eh-pH diagrams

Eh-pH diagrams are applicable to aqueous solution systems and reflect the relationship between potential, pH, and ion activity of different reactions under different conditions [23]. The potential-pH diagram shows the equilibrium conditions and stable regions of different components. It can also be used to judge the directions and limits of different chemical reactions under different conditions [24]. To understand the thermodynamics of vanadium-titanium iron ore concentrate during acid leaching, we performed a thermodynamic analysis of the atmospheric leaching process of vanadium-titanium iron ore concentrate by plotting the Eh-pH diagram of the V-Fe-H_2O system at different temperatures (25 ℃, 50 ℃, 75 ℃, and 100 ℃) in the standard state.

According to the thermodynamic reaction equations and data from each element and leaching agent under the corresponding acid leaching conditions. The ion concentration of V-Fe-H_2O aqueous solution was 0.1 mol/kg. As shown in Figure. 2, the stable regions of soluble V^{3+}, VO^{2+}, and VO_2^+ were all located within the stable regions of Fe^{3+} and Fe^{2+} under acidic conditions. As can be seen from Figure. 2, the redox potential corresponding to the stable zone of soluble vanadium and iron ions gradually increased, and the pH gradually decreased as the temperature increased. Thermodynamic analysis showed that increasing the temperature decreased the leaching of the valuable element vanadium and impurity iron. We also analyzed the effect of temperature on kinetic factors such as the reaction rate. Acid leaching experiment is needed to verify the accuracy of the thermodynamic calculations.

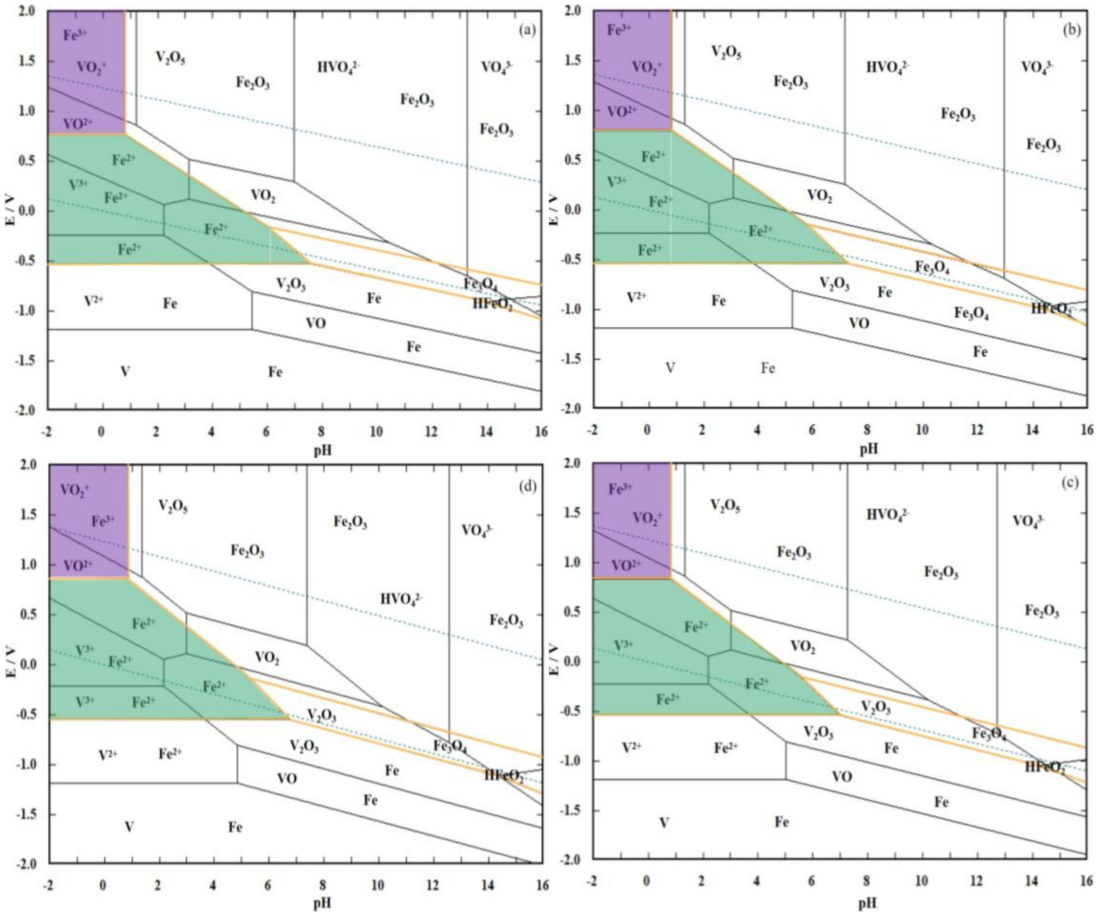

Fig. 2. E-pH diagram of the V-Fe-H_2O system at different temperatures (25 ℃, 50 ℃, 75 ℃ and 100 ℃) in the standard state.

4. Results

4.1 First stage leaching

The lower the solid-to-liquid ratio, the larger the amount of leachate to be processed and the lower the vanadium concentration in the leachate. This situation necessitates the use of multi-stage extraction to precipitate vanadium, which is not suitable for industrial production [25]. At higher solid-liquid ratios, the calcium silicate in the pellet reacts with sulfuric acid to form silicic acid during leaching process. This causes the pellets to be wrapped by silica gel due to the aggregation of silicic acid. This makes the leaching solution difficult to filter,. Therefore, the main purpose of the first stage of leaching was to remove silicon. This stage was further divided into pellet silicon removal and leaching solution silicon removal. The effects of acid concentration and solid-liquid ratio on the formation time of silica gel and the leaching rates of vanadium and iron were investigated during the removal of silicon from the pellet. The effect of acid concentration and standing time on the filtration time of the leaching solution was investigated for removing silicon from the leaching solution. As both the pellets and leachate after silicon removal were filtered, some ferrovanadium was lost. Therefore, a lower leaching rate of V and Fe in the first stage is better.

Silicic acid tends to undergo self-polymerization in solution. In the presence of an acid or salt, silicic acid first self-polymerizes and then forms a three-dimensional reticular gel [26]. The condensation tendency of SiO_2 in acidic ferric salt solution depends on the property and composition of the solution, including the acidity of the solution, the concentration of silicic acid, and the presence of other metal salts.

4.1.1 Effect of acid concentration on pellet silicon removal

The experiment was carried out under a solid-liquid ratio of 6: 1 and room temperature. The influence of acid concentration on the formation time of silica gel and the leaching rate of vanadium and iron is shown in Figure. 3a,c. The silica gel formation time was significantly reduced upon increasing the acid concentration, and the leaching rate of both vanadium and iron increased and then decreased. This was because increasing the acid concentration directly increased the concentration of H^+ in the solution, which increased the number of collisions between H^+ and silicate phase per unit time, thus accelerating the reaction rate. This ultimately increased the silicon removal efficiency per unit time. When the acid concentration reached 1.5 mol/L, there was a significant decrease in the leaching rate of both vanadium and iron. This was because as the acid concentration increased, the silica gel formation time decreased significantly, resulting in a shorter reaction time between the H^+ and vanadium-containing phases in the leachate. This decreased the leaching rate of vanadium and iron. Therefore, the optimal acid concentration during the pellet silicon removal process was 1.5 mol/L.

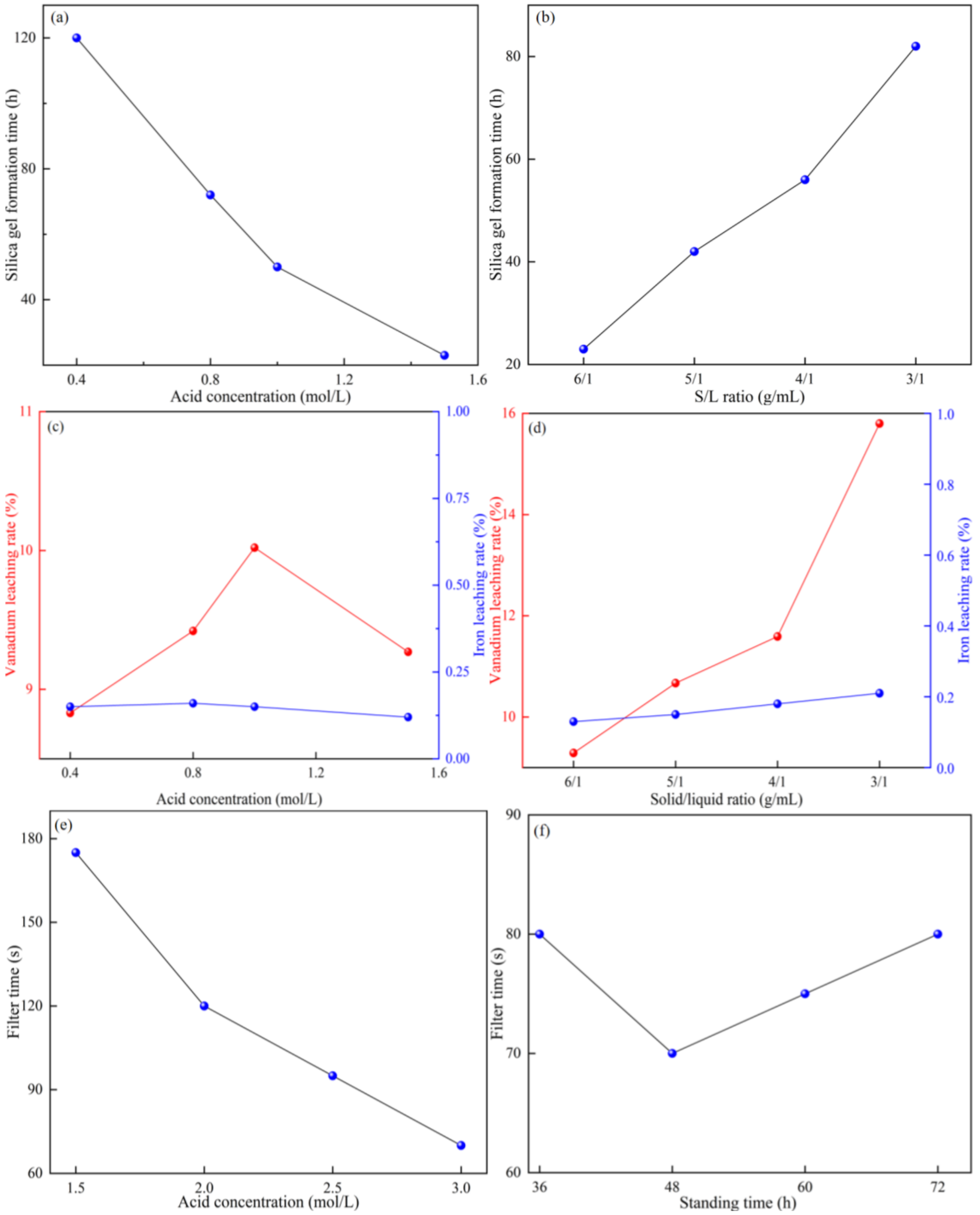

Fig. 3. Effects of (a,c) acid concentration, (b,d) solid-liquid ratio on the formation time of silica gel and leaching rate of vanadium and iron. Effects of (e) acid concentration and (f) standing time on filter time of leachate.

4.1.2 Effect of solid-liquid ratio on silicon removal from pellets

The experiments were carried out at room temperature and an acid concentration of 1.5 mol/L. The effect of the solid-liquid ratio on the formation time of the silica gel and the leaching rate of vanadium and iron is shown in Figure. 3b,d. As the solid-liquid ratio decreased, the silica gel formation time increased significantly because, at a lower solid-liquid ratio, there was a lower silicic acid concentration in the leachate, making it less likely to flocculate into a silica gel. The leaching rates of vanadium and iron increased because, as the solid-liquid ratio increased, the concentration difference of the reactants on both sides of the diffusion layer increased, thus improving the better kinetics. Therefore, the optimal solid-liquid ratio in the pellet during silicon removal was 6: 1.

4.1.3 Effect of acid concentration on silicon removal from the leachate

The influence of the acid concentration on the removal of silicon from the leachate is mainly affected by the filtration time. Experiments were conducted at room temperature with a standing time of 48 h. As shown in Figure. 3e, the filtration time decreased upon increasing the acid concentration. This was because the degree of polymerization of silicic acid increased upon increasing the overall acid concentration of the solution. The higher the degree of polymerization of silicic acid, the easier it was to interact with the flocculant during flocculation to form a mesh structure. Thus, a short silicon removal time was achieved, so the acid concentration chosen for the leach solution silicon removal was 3.0 mol/L.

4.1.4 Effect of standing time on silicon removal from the leachate

The effect of standing time on silicon removal from the leachate is mainly affected by the filtration time. Experiments were carried out at room temperature and an acid concentration of 3.0 mol/L. The results are shown in Figure. 3f. When the resting time was extended from 36 h to 48 h, the required filtration time was shortened from 80 s to 70 s. When the resting time was extended, the filtration time increased. This was because adding a flocculant caused the macromolecular polyelectrolytes to cross-link the colloidal particles into a net-like structure that formed flocculation clusters, thus facilitating filtration. However, upon further extending the resting time, the macromolecular pellets originally formed by flocculation began to decompose, extending the filtration time. Therefore, the resting time of 48 h was optimal.

4.2 Second-stage leaching

The pellets and leachate obtained after the first stage of leaching and silicon removal filtration were subjected to the second stage of leaching.

4.2.1 Effect of acid concentration on the leaching rate of vanadium and iron

The effect of acid concentration on the leaching rate of vanadium and iron was investigated by changing the acid concentration at room temperature, a solid-liquid ratio of 6: 1, and a leaching time of 8 d. As shown in Figure. 4a, the leaching rate of vanadium and iron increased upon increasing the acid concentration. When the concentration increased from 1.0 mol/L to 2.0 mol/L, the leaching rate of vanadium increased rapidly. From 2.0 mol/L to 2.5 mol/L, the leaching rate of vanadium started to increase slowly. Although the iron leaching rate increased, it only increased an additional 0.5%, showing that the acid concentration had little effect on the iron leaching rate. To save costs, the optimal acid concentration was 2.0 mol/L.

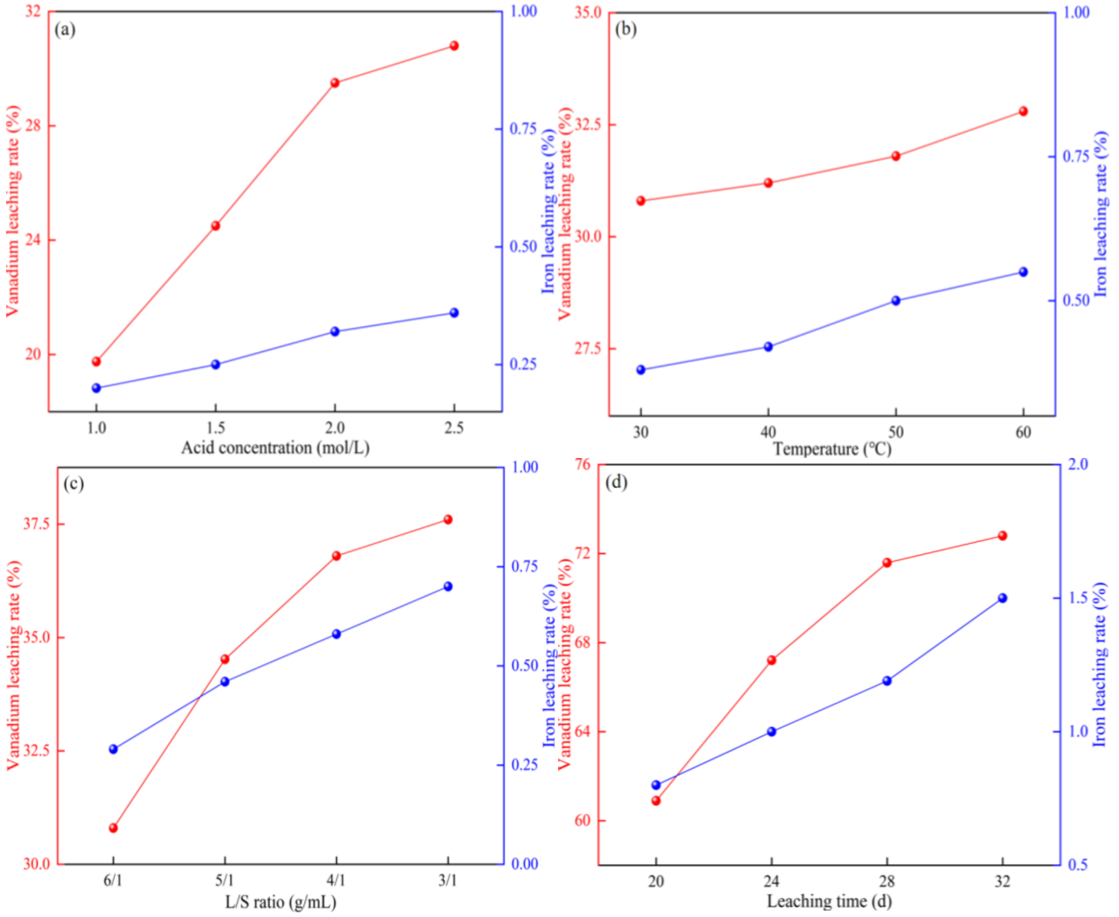

Fig. 4. Effects of (a) acid concentration, (b) temperature, (c) solid-liquid ratio and (d) leaching time on the leaching rate of vanadium and iron.

4.2.2 Effect of temperature on the leaching rate of vanadium and iron

Figure. 4b shows that upon continuously increasing the leaching temperature, the leaching rate of vanadium and iron both slowly increased. The above Eh-pH diagram shows that a higher temperature was detrimental to the leaching of both vanadium and iron. Increasing the temperature significantly increased the energy consumption, so room temperature was finally chosen as the subsequent leaching temperature.

4.2.3 Effect of solid-liquid ratio on the leaching rate of vanadium and iron

As shown in Figure. 4c, when the solid-liquid ratio was increased from 6: 1 to 5: 1, the leaching rate of vanadium was significantly improved. The leaching rate of vanadium continued to slowly increase upon increasing the ratio 5: 1 to 3: 1. Throughout the leaching process, the leaching rate of iron continued to increase, although the increase was limited to within 0.5%. At a solid-liquid ratio of 3: 1, the vanadium concentration of the final leach solution reached 5 g/L, and the maximum vanadium leaching rate was achieved. Therefore, 3: 1 was chosen as the optimal solid-liquid ratio.

4.2.4 Effect of leaching time on the leaching rate of vanadium and iron

As shown in Figure. 4d, the leaching rate of vanadium increased significantly when the leaching time was extended from 20 d to 28 d. The leaching rate of vanadium increased much more slowly upon extending the time from 28 d to 32 d. The iron leaching rate increased steadily throughout the process upon increasing the leaching time. Since a longer leaching time will increase production costs, the optimal leaching time was chosen to be 28 d.

5. Discussion

5.1 Characterization of pellets before and after leaching

Figure. 5 shows the XRD patterns of the pellets before and after leaching. Diffraction peaks of the pellets before and after leaching were attributed to Fe_2O_3 and Fe_9TiO_{15}, which are a result of the combination of vanadium and titanium iron ore concentrates during roasting. This indicates that the leaching process did not change the overall phase composition of the pellets. The faint impurity peaks before and after leaching did not change significantly, indicating that Si, Ca, Mg, Al, Cr, and other impurity metals had limited leaching rates. No diffraction peaks of elemental vanadium were observed in the XRD patterns of the pellets before and after leaching because the vanadium content in CPVC was only 0.3%. The vanadium content of the pellets was further decreased after leaching, so there were no diffraction peaks due to elemental vanadium.

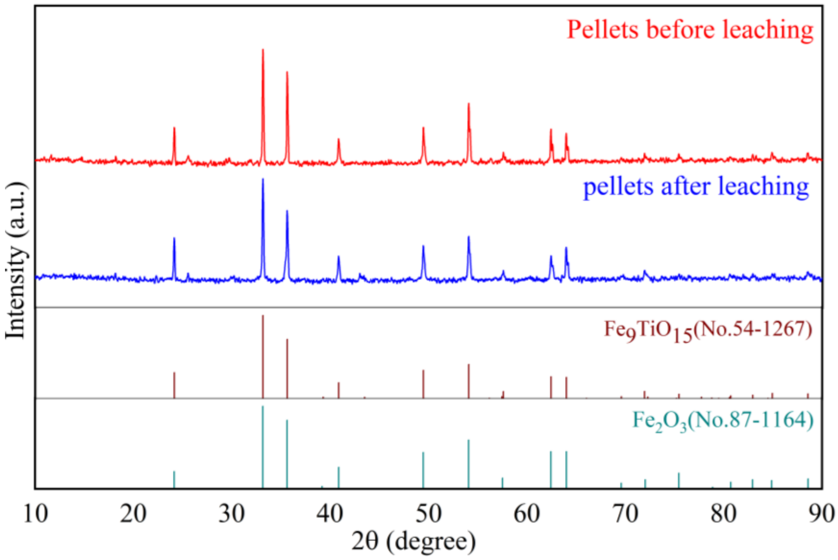

Fig. 5. XRD patterns of before and after leaching pellets.

Figure. 6a shows that almost all vanadium in the pellet before leaching existed as V_2O_5. In the XPS spectrum of V 2p in Figure. 6b, the V_2O_5 peak at a binding energy of 517.1 eV disappeared, and only the faint V_2O_5 peak at 529.6 eV remained. This indicates that most vanadium dissolved in the leachate during sulfuric acid leaching. Figure. 6c shows that the vast majority of Fe in the pellets before leaching existed as Fe_2O_3, accompanied by a small amount of FeO. Figure. 6d shows that the FeO peak at 709.6 eV disappeared, which indicates that divalent iron was almost completely leached. The Fe_2O_3 peaks at 710.8 eV and 724.4 eV were consistent with the peak intensity in Figure. 6c, which indicates that almost no trivalent Fe was leached by sulfuric acid. Since most iron in the roasted pellets existed as trivalent iron, the selective leaching of V and Fe was realized.

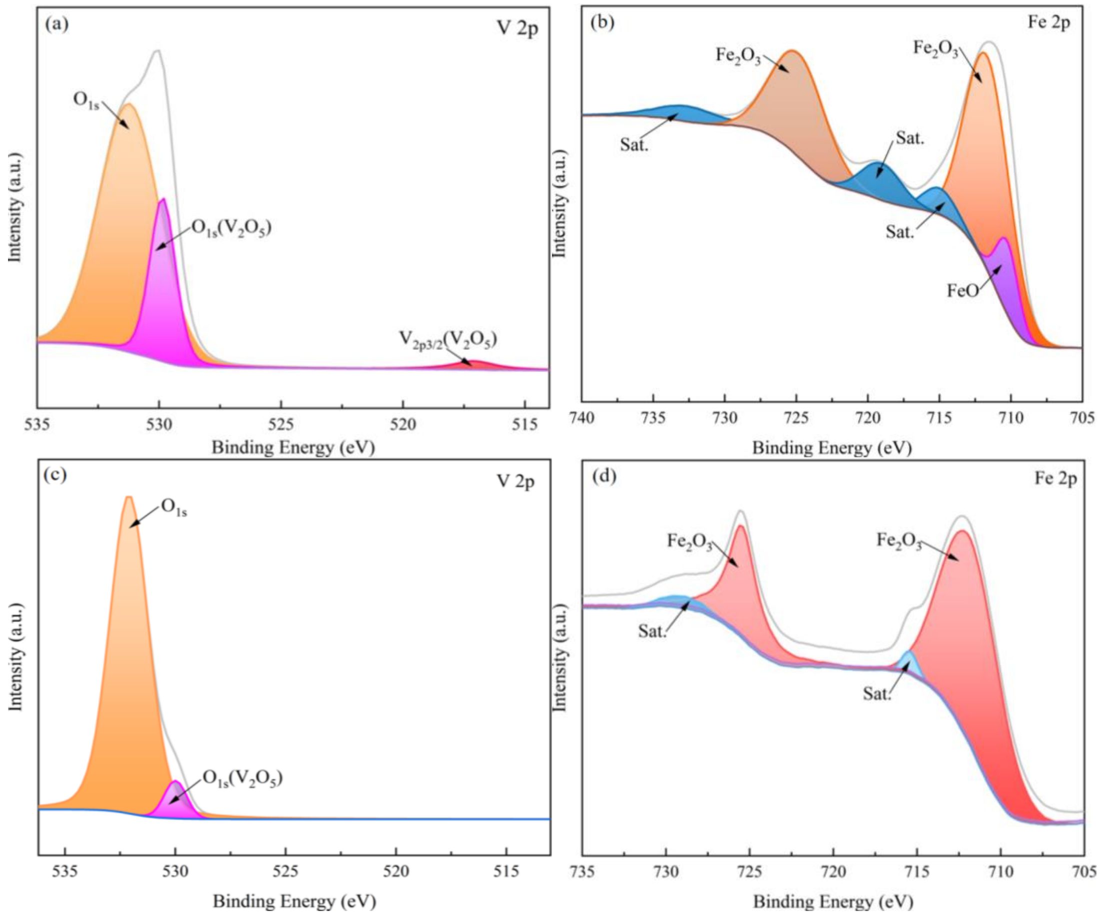

Fig. 6. XPS patterns of (a) V 2p of roasted pellets,(b) Fe 2p of roasted pellets, (c) V 2p of leaching pellets,(d) Fe 2p of leaching pellets.

The morphology and composition of the pellets before and after leaching are shown in Figure. 7a and 8a. It can be seen that the main components of the pellets before and after leaching were Fe, O, Ti, and other elements. V was not detected in any of the samples. Compared with the pellets before leaching, the elemental S content in the pellets after leaching was higher. A highly correlated distribution of Fe, O, and Ti can be seen in the face scan plots of the pellets before and after leaching. This shows that the main phases of the roasted pellets were Fe_2O_3 and Fe_9TiO_{15}, which was consistent with the XRD analysis of the pellets before and after leaching. The very high correlation between the distribution of Si and Ca in Figure. 7b indicates that the roasting temperature of the roasted pellets was too high, and a silicate compound ($Ca_2MgSi_2O_7$) was generated. The high correlation between the distribution of S and Al and Mg in Figure. 8b indicates that S in the leaching pellet entered the pellet through the metal sulfate compounds formed by the reaction of metal oxides in the pellet with sulfuric acid. The leaching pellets were desulfurized by secondary roasting.

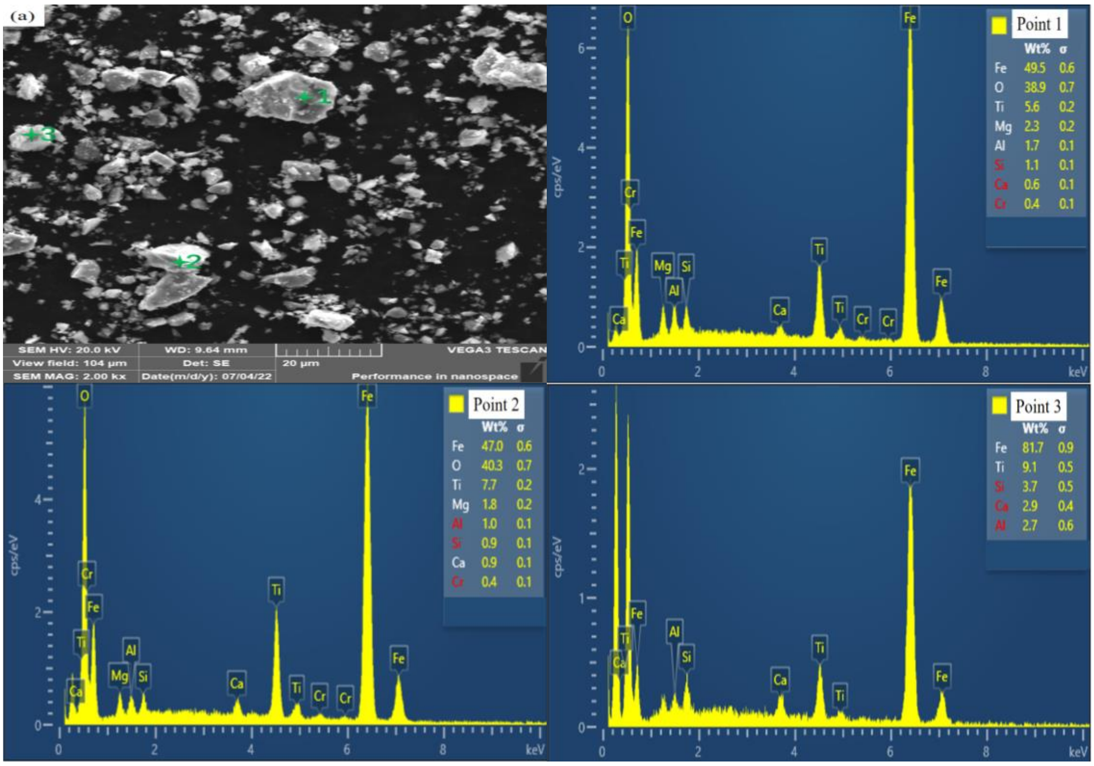

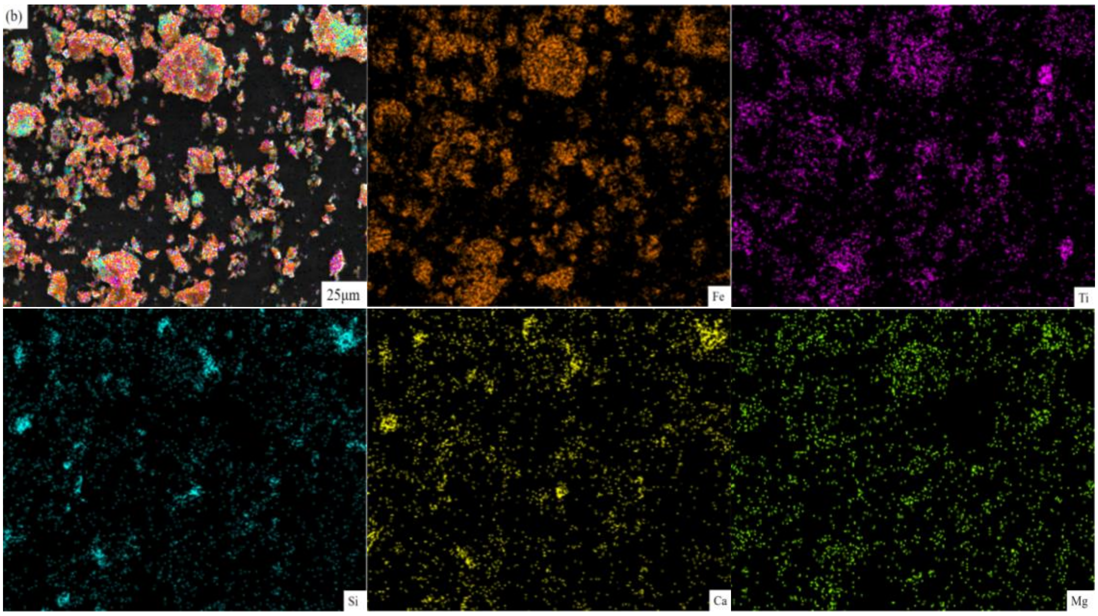

Fig. 7. SEM images of pellets before leaching.

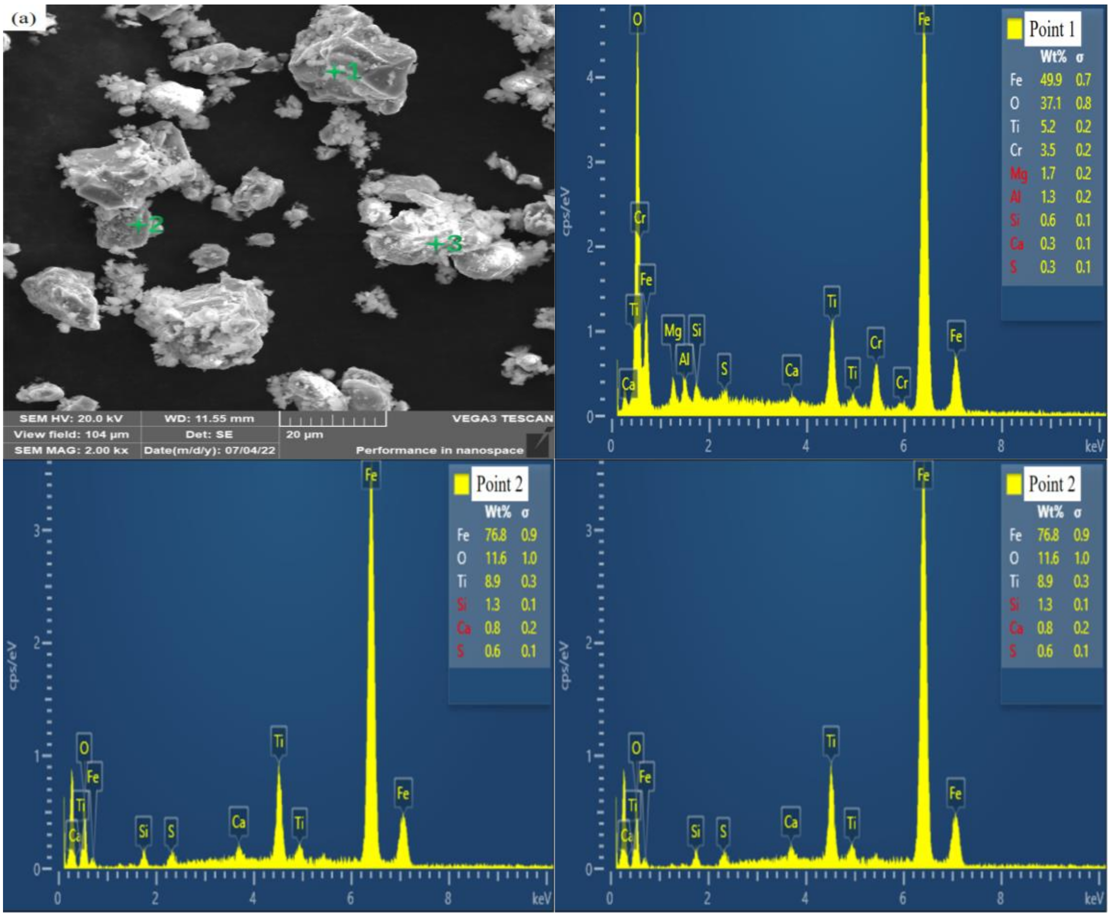

Point 1	Wt%	σ
Fe	49.9	0.7
O	37.1	0.8
Ti	5.2	0.2
Cr	3.5	0.2
Mg	1.7	0.2
Al	1.3	0.2
Si	0.6	0.1
Ca	0.3	0.1
S	0.3	0.1

Point 2	Wt%	σ
Fe	76.8	0.9
O	11.6	1.0
Ti	8.9	0.3
Si	1.3	0.1
Ca	0.8	0.2
S	0.6	0.1

Point 2	Wt%	σ
Fe	76.8	0.9
O	11.6	1.0
Ti	8.9	0.3
Si	1.3	0.1
Ca	0.8	0.2
S	0.6	0.1

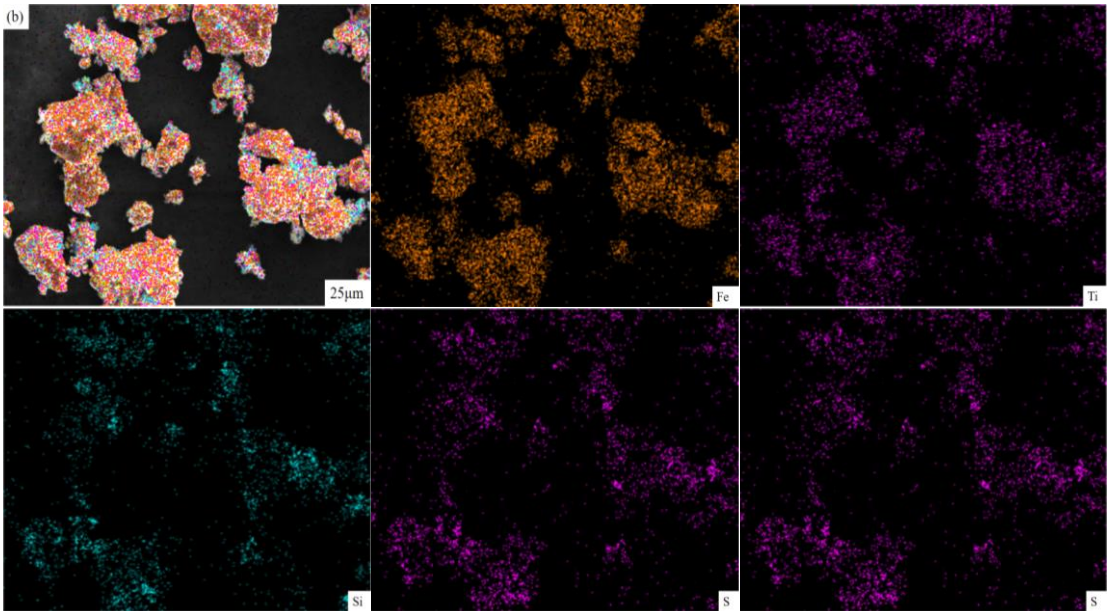

Fig.8. SEM images of pellets after leaching.

As shown in Figure. 9, the crushing strength of the pellets significantly decreased after leaching. After the second roasting stage, the pellet crushing strength exceeded 2000 N again, which meets the requirements of iron making.

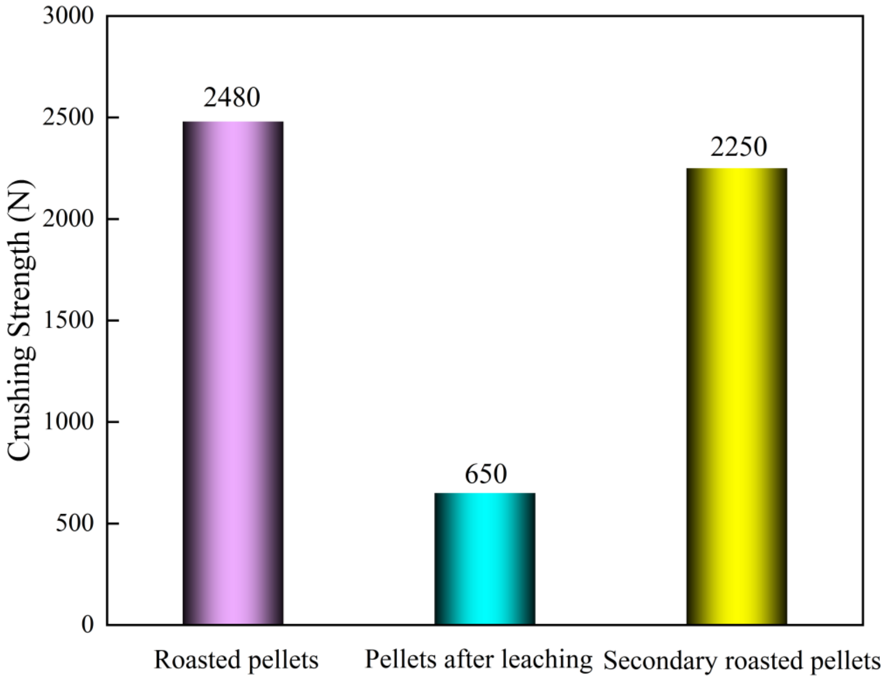

Fig. 9. Pellet crushing strength of roasted pellets, pellets after leaching and secondary roasted pellets.

6. Conclusions

A two-stage selective cycle leaching process of vanadium with sulfuric acid was developed. The results showed that under these optimal conditions， the leaching rates of vanadium and iron were 75.52% and 0.71%, respectively, demonstrating the selective leaching of vanadium and iron. The concentration of vanadium in the leachate reached 6.80 g/L. Vanadium was directly precipitated. After secondary roasting, the crushing strength of the pellets reached 2250 N, which meets the requirements of blast furnace ironmaking. The Eh-pH diagrams of the V-Fe-H_2O system at different temperatures were plotted by thermodynamic calculations. It was demonstrated that the selective leaching of vanadium and iron was thermodynamically difficult to achieve by simply changing the conventional acid leaching conditions. It also shows that compared with the conventional heap leaching of vanadium slag, cyclic leaching of pellets can achieve selective leaching. The main phases in the spheres remained unchanged but the iron grade in the pellets after leaching was slightly increased. S in the sulfuric acid solution entered the leaching pellets through an acid leaching reaction and could be removed by the secondary roasting of the leaching pellets.

References

1 Langeslay, R.; Kaphan, D.; Marshall, C.; Stair, P.; Sattelberger A.; Delferro, M. Catalytic applications of vanadium: a mechanistic perspective. Chem. Rev. **2019**, 119, 2128-2191.

2 Kurtz, R.; Abe, K.; Chernov, V.; Hoelzer, D.; Matsui, H.; Muroga, T.; Odette, G. Recent progress on development of vanadium alloys for fusion. *J. Nucl. Mater.* **2005**, 329-333, 47-55.

3 Parasuraman, A.; Lim, T.; Menictas, C. Review of material research and development for vanadium redox flow battery applications. *Electrochim. Acta*. **2013**, 101, 27-40.

4 Moskalyk,R.; Alfantazi, A. Processing of vanadium: a review. *Miner. Eng.* **2003**, 16, 793-805.

5 Guo, Y.; Li, H.; Huang, J.; Shen, S.; Wang, C.; Wu, Z.; Xie, B. Efficient separation of V (V) and Cr (VI) in aqua by microemulsion extraction. *Sep. Purif. Technol.* **2020**, 238, 116409.

6 G. Wang, M. M. Lin, J. Diao, H. Y. Li, B. Xie and G. Li, Novel strategy for green comprehensive utilization of vanadium slag with high-content chromium. *Acs. Sustain. Chem. Eng.* **2019**, 7, 18133-18141.

7 Bian, Z.; Feng, Y.; Li, H. Efficient separation of vanadium, titanium, and iron from vanadium-bearing titanomagnetite by pressurized pyrolysis of ammonium

chloride-acid leaching-solvent extraction process. *Sep. Purif. Technol.* **2021**, 255, 117169.

8 Gao, H.; Jiang,T.; Xu,Y.; Wen, J.; Xue, X. Leaching kinetics of vanadium and chromium during sulfuric acid leaching with microwave and conventional calcification-roasted high chromium vanadium slag. *Miner. Process. Extr. M.* **2020**, 41, 22-31.

9 Li, R.; Liu, T.; Zhang, Y.; Huang, J.; Xu, C. Efficient Extraction of Vanadium from Vanadium-Titanium Magnetite Concentrate by Potassium Salt Roasting Additives. *Minerals-basel.* **2018**, 8, 25.

10 Zou, K.; Xiao, J.;;Liang, G.; Huang, W.; Xiong, W. Effective extraction of vanadium from bauxite-type vanadium ore using roasting and leaching. *Metals-basel.* **2021**, 11, 9.

11 Xiang, J.; Huang, Q.; Lv, X.; Bai, C. Extraction of vanadium from converter slag by two-step sulfuric acid leaching process. *J. Clean. Prod.* **2018**, 170, 1089-1101.

12 Peng, H. A literature review on leaching and recovery of vanadium(Review). *J. Environ. Chem. Eng.* **2019**, 7, 103313.

13 Li, M.; Liu, B.; Zheng, S.; Wang, S.; Du, H.; Dreisinger, D.; Zhang, Y. A cleaner vanadium extraction method featuring non-salt roasting and ammonium bicarbonate leaching. *J. Clean. Prod.* **2017**, 149, 206-217.

14 Liu, S.; Ding, E.; Ning, P.; Xie, G.; Yang, N. Vanadium extraction from roasted vanadium-bearing steel slag via pressure acid leaching. *J. Environ. Chem. Eng.* **2021**, 9, 105195.

15 Peng, H.; Guo, J.; Zhang, X. Leaching Kinetics of Vanadium from Calcium-Roasting High-Chromium Vanadium Slag Enhanced by Electric Field. *Minerals-basel.* **2020**, 5, 17664-17671.

16 Vaschetti, V.; Eimer, G.; Cánepa, A.; Casuscelli, S. Catalytic performance of V-MCM-41 nanocomposites in liquid phase limonene oxidation: Vanadium leaching mitigation. *Micropor. Mesopor. Mat.* **2021**, 311, 110678.

17 Xiang, J.; Wang, X.; Pei,G. Recovery of vanadium from vanadium slag by composite roasting with CaO/MgO and leaching. *T. Nonferr. Metal. Soc.* **2020**, 30, 11.

18 Zhang, J.; Zhang, W.; Xue, Z. An Environment-Friendly Process Featuring Calcified Roasting and Precipitation Purification to Prepare Vanadium Pentoxide from the Converter Vanadium Slag. *Metals-basel.* **2019**, 9, 21.

19 Wen, J.; Jiang, T.; Wang, J.; Lu, L.; Sun, H. Cleaner extraction of vanadium from vanadium-chromium slag based on MnO2 roasting and manganese recycle. *J. Clean. Prod.* **2020**, 261, 121205.

20 Zhang, Y.; Zhang, T.; Dreisinger, D.; Lv, C.; Lv, G.; Zhang, W. Recovery of vanadium from calcification roasted-acid leaching tailing by enhanced acid leaching. *J. Hazard. Mater.* **2019**, 369, 632-641.

21 Wen, J.; Jiang, T.; Zhou, W.; Gao, H.; Xue, X. A cleaner and efficient process for extraction of vanadium from high chromium vanadium slag: Leaching in (NH4)(2)SO4-H2SO4 synergistic system and NH4+ recycle. *Sep. Purif. Technol.* **2019**, 216, 126-135.

22 Hu, P.; Zhang, Y.; Huang, J.; Liu, T.; Yuan, Y.; Xue, N. Eco-Friendly Leaching and Separation of Vanadium over Iron Impurity from Vanadium-Bearing Shale Using Oxalic Acid as a Leachant. *Acs. Sustain. Chem. Eng.* **2018**, 6, 1900-1908.

23 Cao, Z.; Ma, B.; Wang, C.; Chen, Y.; Liu, B.; Xing, P.; Zhang, W. E-pH diagrams for the metal-water system at 150 ° C: Thermodynamic analysis and application for extraction and separation of target metals from saprolitic laterite(Article). *Miner. Eng.* **2020**, 152, 106365.

24 Pesterfield, L.; Maddox, J.; Crocker, M.; Schweitzer, G. Pourbaix (E–pH-M) Diagrams in Three Dimensions. *J. Chem. Educ.* **2012**, 89, 891-899.

25 Chen, D.; Zhao, H.; Hu, G.; Qi, T.; Yu, H.; Zhang, G.; Wang, L.; Wang, W. An extraction process to recover vanadium from low-grade vanadium-bearing titanomagnetite. *J. Hazard. Mater.* **2015**, 294, 35-40.

26 Deng, S.; Zheng, W. Effect of polymeric flocculants in secondary removal of silicon for high-purity zirconium oxychloride preparation. *Yingyong. Huaxue*. **1999**, 16.